

Laser Photolysis Study of the Photoisomerization of Retinals

Bernard Veyret, Stephen G. Davis, Masayoshi Yoshida, and Karl Weiss*¹

*Contribution from the Photochemistry and Spectroscopy Laboratory,
Department of Chemistry, Northeastern University, Boston, Massachusetts 02115.
Received August 15, 1977*

Abstract: Using pulsed laser photolysis at 347 nm it was shown that the transient absorption of 11-*cis*-retinal is due to the triplet state of this isomer as well as that of *all-trans*-retinal. The triplet spectra of both isomers have been constructed in the 300–500-nm region, and their intersystem crossing yields have been determined by an energy extrapolation procedure. The laser photolysis method was also used to determine the photoisomerization quantum yields for 11-*cis*-retinal ($\phi_{\text{isom}} = 0.25 \pm 0.03$) and *all-trans*-retinal ($\phi_{\text{isom}} = 0.07 \pm 0.03$) in hexane. The laser-stimulated room temperature emission spectra of *all-trans*-, 13-*cis*-, and 11-*cis*-retinal have been measured, and the quantum yields of these emissions have been estimated. Information about the photoisomerization pathway of 11-*cis*-retinal was obtained from absorption measurements in two spectral regions at various energies and times after excitation. Based on the insensitivity of ϕ_{isom} to oxygen, the evident lack of ground-state *all-trans*-retinal production during the initial ~50-ns time interval, and quantitative calculations based on kinetic models, it is concluded that isomerization in hydrocarbon solvents occurs predominantly from an internally excited first triplet state. Evidence was found for a biphotonic contribution to the isomerization.

It is by now well established that the visual pigment rhodopsin consists of the chromophore 11-*cis*-retinal bound to the protein opsin by means of a protonated Schiff base linkage.^{2–5} Photolysis of rhodopsin ultimately produces opsin and retinal, with the latter now in the *all-trans* configuration.⁶ The nature of the intermediates involved in this bleaching reaction of rhodopsin has been widely studied from experimental and theoretical points of view.⁷ Although the protein moiety clearly plays an important role in this transformation, much of the attention has focused on the behavior of model compounds, particularly that of the retinal isomers.⁸

The photoisomerization of retinals has been investigated in numerous laboratories.^{9–14} These studies have included the measurement of photoisomerization quantum yields for the direct excitation^{9,11,13} and triplet-sensitized^{10,11,13} processes, the determination of isomer distributions,^{13,14} and laser photolysis experiments.¹² Unfortunately, few unequivocal mechanistic conclusions have resulted from these efforts. In particular, the question whether isomerization by direct excitation under a given set of conditions involves excited singlet and/or triplet pathways remains unanswered.

That triplet states may play a significant role in the photoisomerization of retinals follows from the relatively high intersystem crossing quantum yields (~ 0.5)^{11,15–17} in nonpolar solution.¹⁸ Photosensitization experiments with biacetyl and biphenyl as triplet energy donors have provided isomerization quantum yields (ϕ_{isom}) from the retinal triplet states of 0.15–0.2 for the 11-*cis*-, 13-*cis*-, and 9-*cis*-to *all-trans* isomer processes.^{11,13,19} Taken at face value in conjunction with the quantum yields for the direct isomerization process, these data indicate a substantial contribution ($\sim 30\%$) from the triplet pathway to the direct process.¹³ The recent proposal that the isomeric retinal triplet states are rapidly equilibrated prior to their decay²⁰ also appears to argue for triplet state participation in the direct photoisomerization.

The situation is, however, not quite so simple. Although the 11-*cis*-retinal triplet state is efficiently quenched by oxygen, Rosenfeld et al.¹¹ have reported that ϕ_{isom} for both the direct and photosensitized processes is unaffected by this gas. These observations led the authors to propose that, in the sensitized reaction, isomerization occurs in a thermally excited triplet state which decays with partitioning into relaxed *cis* and *trans* triplet configurations. Whether or not the same mechanism is operative for the direct photoisomerization of 11-*cis*-retinal could not be inferred from the sensitized case. Menger and Kligler¹² have examined the direct process for 11-*cis*-retinal by the laser flash photolysis technique. Based on the finding

that, in nonpolar solution, the rates of recovery of ground-state absorption and triplet decay are equal, they conclude that isomerization does occur from a thermally relaxed triplet level in this medium. For polar solution, where a different kinetic behavior was observed, a predominantly singlet pathway was proposed.¹²

The seemingly contradictory evidence from the quantum yield¹¹ and kinetic spectroscopy^{12,20} experiments represents the point of departure for the present study. With the distinction between various photoisomerization pathways as our aim, we have employed the laser photolysis technique to carefully reexamine the transient spectroscopy of 11-*cis*-retinal and *all-trans*-retinal in the nanosecond time domain. In addition, the intersystem crossing quantum yields, photoisomerization quantum yields, and laser-stimulated emission have been measured for these compounds. A novel aspect of this study is the use made of the nonlinear variation of transient and isomeric product absorptions with the laser excitation energy. This approach proved to be a particularly fruitful source of photochemical and photophysical information.

Experimental Section

Materials. *all-trans*-Retinal, 13-*cis*-retinal (Sigma Chemical Co.), and 11-*cis*-retinal (gift of Hoffmann-La Roche, Inc.), which had absorption spectra in agreement with those reported,^{9,17} were used as received. The samples were stored at -20°C . Anthracene (Aldrich Chemical Co., zone refined) and rhodamine 6-G (Phase-R Corp.) were also used without further purification.

For the transient absorption experiments, the solvents cyclohexane, hexane (Burdick and Jackson), absolute ethanol (U.S. Industrial Chemical Co.), and methanol (Fisher, "Spectrograde") were used as received. For the laser-stimulated emission work, the hydrocarbon solvents were purified by treatment with fuming sulfuric acid (10%), refluxing with basic potassium permanganate solution, and fractional distillation from calcium hydride. The methanol was refluxed with, and then distilled from, magnesium powder. These procedures yielded solvents which showed acceptable levels of background emission ($<5\%$ above 420 nm) in relation to the sample emission with laser excitation.

Apparatus and Methods. The basic laser photolysis apparatus, which provides 347-nm light pulses of ca. 25-ns duration, has been previously described.^{16,21,22} A recent modification consists of reversal of the operating mode of the Pockels cell (Lasermetrics, Inc.) in order to protect this device against damage by continuous high voltage. For the emission experiments, a Bausch and Lomb high-intensity monochromator (33-86-02) fitted with appropriate filters and an RCA 8852 photomultiplier tube was used with a 10-nm bandpass. The spectral response of this combination was determined with a standard lamp (GE Q6.6/T4/CL).²³

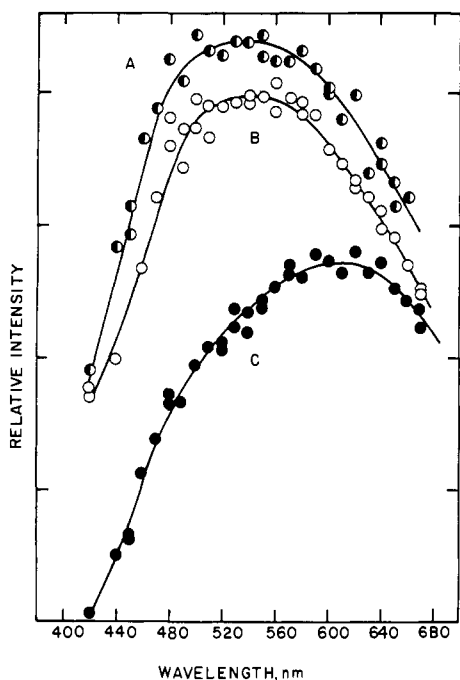


Figure 1. Room temperature, laser-stimulated emission in cyclohexane, 22 mJ/pulse, of 7.5×10^{-6} M *all-trans*-retinal (A), 1.25×10^{-5} M 13-*cis*-retinal (B), and 8.8×10^{-6} M 11-*cis*-retinal (C). The relative positions of the curves on the intensity scale are arbitrary.

In the laser-stimulated emission measurements, appropriate corrections were applied for pulse energy variations, nonlinear absorption effects, and absorption due to the triplet state. Estimates of the fluorescence quantum yields were obtained by comparing the areas under the corrected retinal emissions with those for the reference compounds anthracene ($\phi_f = 0.30$ in ethanol^{24a}) and rhodamine 6-G ($\phi_f = 0.84$ in ethanol²⁵). The intersystem crossing quantum yields (ϕ_{isc}) and photoisomerization quantum yields (ϕ_{isom}) were determined by the comparison method.^{16,22,26}

$$\phi_x = \phi_{isc}^{ref} \frac{I_{abs}^{ref} \epsilon_T^{ref} \Delta D_x}{I_{abs} \Delta \epsilon \Delta D_T^{ref}} \quad (1)$$

Here $x = isc$ or $isom$, ΔD are the changes in optical density measured at appropriate wavelengths, ϵ represents the molar extinction coefficients, and I_{abs} the intensities of absorbed laser radiation. Anthracene, with $\phi_{isc}^{ref} = 0.71$ and $\epsilon_T^{ref}(423 \text{ nm}) = 6.47 \times 10^4 \text{ M}^{-1} \text{ cm}^{-1}$ in cyclohexane,^{26,27} was used as the reference compound for both types of yield. The symbol $\Delta \epsilon$ refers to the difference between the extinction coefficients of the initial and product retinals in case of isomerization, and to the difference between these parameters for the triplet and ground state retinals for intersystem crossing. Measurements of ΔD_x were made at 445–450 nm for the triplet states and at 365–370 nm for isomerization. Values of ϵ_T for the retinals were determined at high laser excitation energies such that the ground states are totally depleted.

The sample solutions were degassed by repeated freeze–pump–thaw cycles in a transfer assembly which permits multiple fillings of the flash cell.²⁸ The ground-state absorption spectra were measured with a Cary 14 spectrophotometer. Unless otherwise indicated, all photolysis experiments were conducted at room temperature, $20 \pm 2^\circ \text{C}$.

Data on the variation of transient and isomeric product absorption with the laser power were evaluated with the aid of an appropriate kinetic model and numerical calculations.^{22,29} The computer program used for this purpose has been modified to include the experimentally determined spatial energy distribution of the laser beam, and to permit computation of ΔD_x values at pertinent wavelengths and time intervals after excitation.

Results

1. Room Temperature Emission. Early in our laser photolysis experiments we noticed that, in the 420–750-nm region, the oscilloscope traces on nanosecond time scales with high gain displayed signals which correspond to emission. It was easily

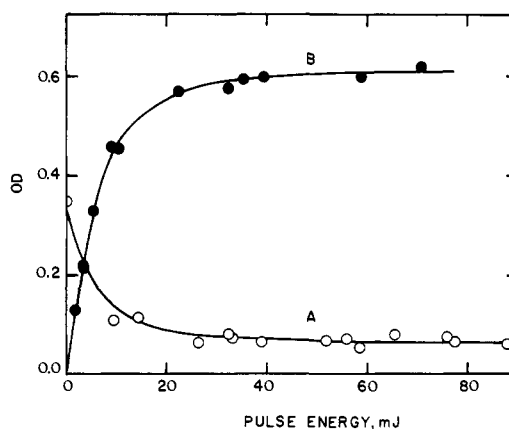


Figure 2. Variation of optical density (OD) with laser power for *all-trans*-retinal (8.75×10^{-6} M) in cyclohexane. (A) OD at 347 nm in aerated solution, determined directly from the energy loss of the laser pulse; (B) OD at 450 nm in degassed solution, measured 50 ns after excitation.

Table I. Emission Data for Retinals

Isomer	Solvent ^a	λ_{max} , nm		$\phi_f \times 10^4$	
		295 K ^b	77 K	295 K ^b	77 K ^d
<i>all-trans</i> -	HC	530	520 ^c	1	50
	MeOH	640	620 ^c	40	
13- <i>cis</i> -	HC	550	505 ^d	0.8	240
	MeOH	640		40	
11- <i>cis</i> -	HC	610		0.9	
	MeOH	640		40	

^a HC is cyclohexane at 295 K and 3-methylpentane at 77 K, both conventionally dried; cf. ref 30. ^b Laser excitation at 347 nm; λ_{max} values ± 30 nm in cyclohexane and ± 40 nm in methanol; ϕ_f values $\pm 50\%$. ^c Reference 30; 213 K in MeOH. ^d Reference 31; excitation at 340 nm.

established that these signals did not originate from stray light. Using compounds with well-characterized emission properties (9,10-diphenylanthracene, rhodamine 6-G) it was found that 347-nm laser excitation can accurately reproduce their fluorescence spectra^{24b} under conditions which correspond to effective quantum yields of $< 10^{-4}$. With the efficacy of the method established, measurements were performed with *all-trans*-retinal, 11-*cis*-retinal, and 13-*cis*-retinal (Figure 1). These emission spectra are characterized by broad, structureless bands. The scatter of the experimental points notwithstanding, it is evident that each isomer gives rise to a distinct spectrum in cyclohexane. The emissions of the three retinal isomers were also measured in methanol, where the broad bands all show maxima at 640 ± 40 nm. A summary of the emission results and a comparison with low-temperature data are given in Table I.

2. Nonlinear Laser Power Effects. During earlier laser photolysis experiments with *all-trans*-retinal¹⁶ it was observed that the optical density of solutions at the laser wavelength (347 nm) decreased rapidly with increasing pulse energy.²⁹ This saturation of absorption, which signifies a major deviation from Beer's law, and the variation of the transient optical density at 450 nm (which represents the triplet state population, vide infra), are shown in Figure 2. Although analogous behavior is shown by all three isomers, the detailed shapes of the curves are quite characteristic for each of them. Figure 3 shows the corresponding curves for 11-*cis*-retinal, as well as the variation of the optical density at 365 nm measured after complete decay of the triplet state; this absorption reflects the isomerization to predominantly *all-trans*-retinal.¹³ At high energy, triplet state production reaches a limit.

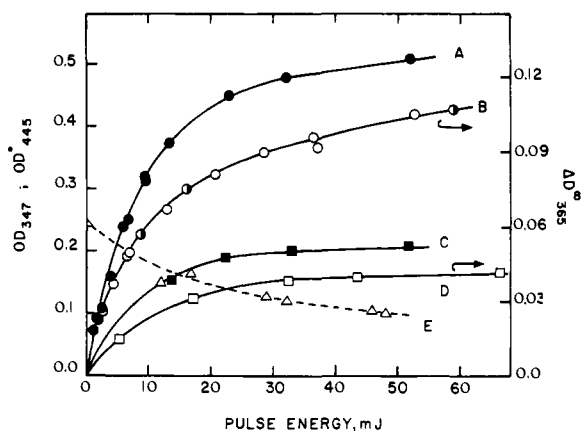


Figure 3. Variation of optical density with laser power for 11-*cis*-retinal. (A) OD at 445 nm, 50 ns after excitation, and (B) change in optical density (ΔD) at 365 nm after triplet decay for 1.0×10^{-5} M retinal in degassed *n*-hexane; (●) designates points measured in aerated solution. (C) OD at 445 nm, and (D) ΔD at 365 nm for 3.8×10^{-6} M retinal in degassed *n*-hexane. (E) OD at 347 nm for 1.0×10^{-5} M retinal in aerated cyclohexane, measured as explained in Figure 2.

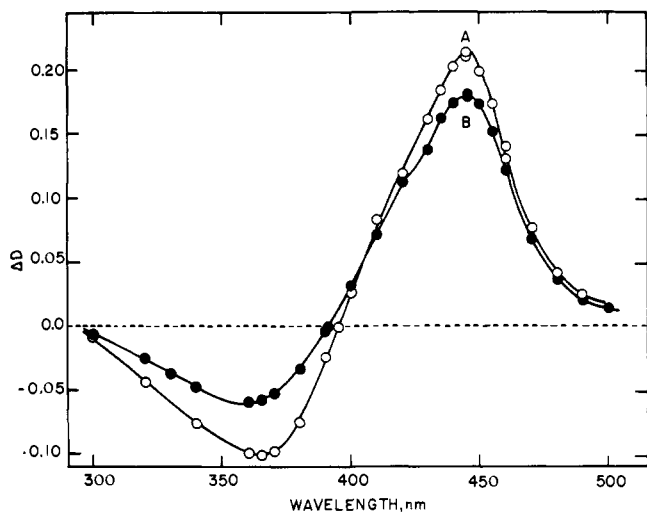


Figure 4. Transient absorption of *all-trans*-retinal (A) and 11-*cis*-retinal (B), 3.4×10^{-6} M solution in degassed *n*-hexane, measured with >50 mJ laser pulse energy.

The bleaching of the retinal solutions at 347 nm is due to the efficient production of triplet state molecules,^{11,16,17} which have much smaller absorption cross sections at this wavelength than do the ground-state molecules (vide infra). The absorption variations with the laser power will be seen to provide important insights into the photoisomerization mechanism.

3. Transient Spectra. The transient absorption spectra of *all-trans*- and 11-*cis*-retinal in *n*-hexane solution are shown in Figure 4. At wavelengths >400 nm, they may be compared with previously reported spectra in several hydrocarbon solvents.^{11,16,20,32} By working in very dilute solution ($\sim 3 \times 10^{-6}$ M) and with energies at which the ground-state population is totally depleted, spectra encompassing the bleaching region (300–400 nm) were obtained from which triplet extinction coefficients could be determined (cf. Discussion section).

Since they will play an important role in the interpretation of the data, we display at this point, in Figure 5, some oscilloscope traces recorded for a hexane solution of 11-*cis*-retinal in the isosbestic region (395–400 nm, Figure 5), where the ground state and triplet state absorptions are of comparable magnitude. At these wavelengths both of these species absorb quite strongly. The trace at 397 nm is particularly significant.

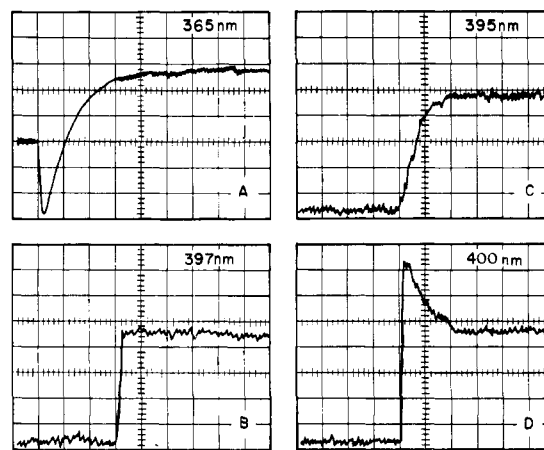


Figure 5. Oscilloscope traces for 11-*cis*-retinal in *n*-hexane. (A) At 365 nm in degassed 3.8×10^{-6} M solution; (B) at 397 nm, (C) at 365 nm, and (D) at 400 nm in aerated 1.3×10^{-5} M solution. The time base is $10 \mu\text{s}/\text{cm}$ for (A) and $100 \text{ ns}/\text{cm}$ for the other traces; the vertical scale is 3.3% absorption/cm in each case. The same traces on longer time scales are observed at 395–400 nm in degassed solution.

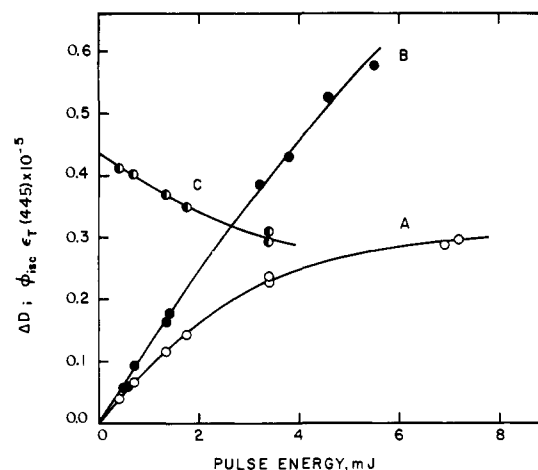


Figure 6. Determination of ϕ_{isc} for *all-trans*-retinal in *n*-hexane. (A) ΔD at 450 nm, 6.1×10^{-6} M retinal; (B) ΔD at 423 nm for 1.0×10^{-4} M anthracene in degassed cyclohexane; (C) product $\phi_{isc} \epsilon_T(445)$ computed with eq 1.

Here, the optical density increase is produced during the excitation pulse and then remains constant with time.

4. Intersystem Crossing Quantum Yields. The determination of these yields is based on eq 1, which is used to compute the product $\phi_{isc} \epsilon_T(445)$. The key to obtaining reliable ϕ_{isc} values which do not incorporate errors due to nonlinear absorption and multiple excitation effects¹⁶ is an extrapolation to zero energy.²² The raw data which enter into the ϕ_{isc} determination for *all-trans*-retinal, and their treatment by eq 1, are shown in Figure 6. With $\epsilon_T(445) = (7.0 \pm 0.7) \times 10^4 \text{ M}^{-1} \text{ cm}^{-1}$ (vide infra), the result is $\phi_{isc} = 0.62 \pm 0.05$ in hexane. This value may be compared with other recent ϕ_{isc} estimates of 0.43,¹⁷ 0.54,¹⁶ 0.60,¹⁵ and 0.70.¹¹ Of course, the ϕ_{isc} results are very sensitive to ϵ_T at λ_{max} , for which values in the range $6.9\text{--}7.8 \times 10^4 \text{ M}^{-1} \text{ cm}^{-1}$ have been previously reported.^{11,15–17}

By the same extrapolation procedure, $\phi_{isc} = 0.50 \pm 0.03$ has been determined for 11-*cis*-retinal in hexane. In the Discussion section it will be shown that 11-*cis*-retinal produces the *all-trans* as well as its own triplet state. Consequently, the above ϕ_{isc} value, which is based on an effective triplet extinction coefficient (cf. Figure 7), refers to the total triplet state production from the 11-*cis* isomer. Previous values of ϕ_{isc} for 11-*cis*-retinal are 0.51¹⁷ and 0.6,¹¹ based on $\epsilon_T(\lambda_{max}) = 6.2 \times 10^4$ and $7.5 \times 10^4 \text{ M}^{-1} \text{ cm}^{-1}$, respectively.

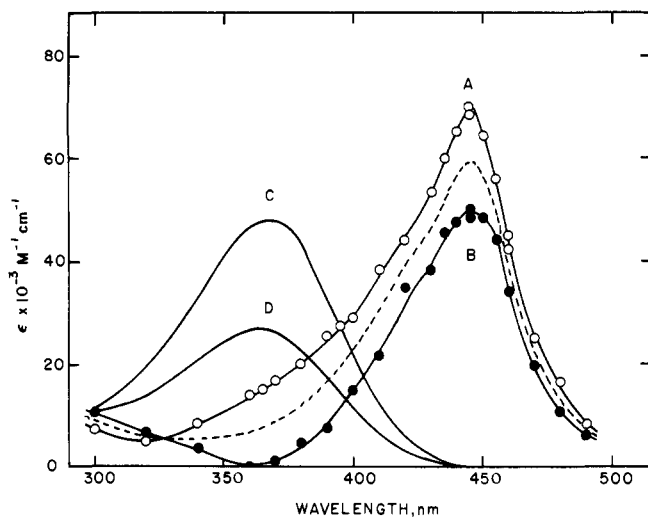


Figure 7. Absorption spectra in *n*-hexane. (A) *all-trans*-retinal triplet state, (B) 11-*cis*-retinal triplet state; (C) and (D) are the corresponding ground-state spectra. The broken curve represents the "effective" triplet state spectrum of the 11-*cis* isomer; see text.

We have also redetermined ϕ_{isc} for *all-trans*-retinal in methanol at room temperature, and confirm that it is much smaller in this solvent than it is in hydrocarbon solution. The new, extrapolated value is 0.11 ± 0.03 , compared with 0.08 previously reported.¹⁶ Interestingly, ϕ_{isc} in methanol appears to increase significantly with decreasing temperature. Thus, preliminary experiments indicate the lower limit of ϕ_{isc} at -60°C to be 0.16.

5. Photoisomerization Quantum Yields. In the application of the energy extrapolation procedure described above to the determination of ϕ_{isom} , the pertinent measurement is the change in optical density at 365 nm after complete decay of the triplet absorption ($t > 100 \mu\text{s}$). This information is utilized in conjunction with the extinction coefficients of the initial and product retinal isomers⁹ (eq 1). A complication arises from the fact that the primary isomerization products in hydrocarbon solution are *all-trans*- and 11,13-*di-cis*-retinal (ratio 5:1) from 11-*cis*-retinal,¹³ and 13-*cis*- and 9-*cis*-retinal (ratio 4:1) from the *all-trans* isomer.¹⁴ In principle, separate quantum yields for each product isomer could be computed since their relative abundances are known. Mitigating against this approach are the close similarity between the spectra of the 9-*cis* and 13-*cis* isomers⁹ and the absence of reliable spectral data for 11,13-*di-cis*-retinal.¹³ For the isomerization of 11-*cis*-retinal, the uncertainty in ϕ_{isom} introduced by assuming the *all-trans* isomer to be the only product is quite small. For *all-trans*-retinal, the error in the total quantum yield is negligible.

Based on data similar to those displayed in Figure 6, the extrapolated value for 11-*cis*-retinal in hexane derived from several such experiments is $\phi_{isom} = 0.25 \pm 0.03$. This result is in excellent agreement with $\phi_{isom} = 0.24 \pm 0.04$ determined by Waddell et al.¹³ with the conventional continuous irradiation method. Earlier reported values are smaller (0.2 ,⁹ 0.12 ± 0.01 ¹¹). We are able to confirm directly by our laser method that ϕ_{isom} for 11-*cis*-retinal is unaffected by oxygen¹¹ (cf. Figure 3).

For *all-trans*-retinal in hexane, the changes in optical density at 365 nm are quite small ($< 5 \times 10^{-3}$) in the low-energy region of interest; consequently, the uncertainty in ϕ_{isom} is larger than in the case of the 11-*cis* isomer. The value obtained, $\phi_{isom} = 0.07 \pm 0.03$, agrees well with all but one previous estimate (0.2 ,⁹ 0.10 ± 0.01 ,¹¹ 0.04 ± 0.01 ,¹³ 0.08 ± 0.02 ¹⁴).

Discussion

The room temperature emission results (Figure 1, Table I) demonstrate the utility of pulsed laser techniques for emission studies of systems with very low quantum yields. A distinct advantage of this technique is the flexibility it provides to examine the influence of environmental factors. The room temperature emission of *all-trans*- and 13-*cis*-retinal has not previously been fully characterized. Moreover, emission from 11-*cis*-retinal has not been detected under any conditions.³¹ In cyclohexane, ϕ_f for the retinals was measured to be $\sim 10^{-4}$; the error in these values is large owing to the relatively small signal-to-noise ratio at some wavelengths and the need to extrapolate bands to determine the areas under them. The emission maximum of 11-*cis*-retinal in cyclohexane is shifted by 60–80 nm relative to the maxima of the *all-trans* and 13-*cis* isomers. Thus, a thermally relaxed excited singlet state with configurational integrity exists for 11-*cis*-retinal and, as for the other isomers, a radiative decay channel is open to this state. Since the differences between the emission spectra of the isomers are maintained even at high excitation energies, interconversion between them may not occur in the excited singlet state. In methanol, the accuracy of our measurements was insufficient to reveal significant differences between the emissions of the three isomers (Table I). In this solvent at room temperature, the quantum yield is more than an order of magnitude larger ($\phi_f \approx 4 \times 10^{-3}$) than it is in cyclohexane.

A noteworthy feature of the emission spectra of *all-trans*- and 13-*cis*-retinal is their substantially greater width at room temperature than at 77 K.³³ The band half-width (cm^{-1}) ratios are ca. 1.6 for *all-trans*-retinal and 1.3 for the 13-*cis* isomer. These results substantiate the importance of conformational freedom in the retinals. The recent report of Takemura et al.³⁰ that no fluorescence was detected from *all-trans*- and 13-*cis*-retinal in absolutely dry alkane solvents at 77 K may indicate that the cyclohexane used in our experiments contained traces of water.

We have also demonstrated that the laser photolysis method can be used to determine photoisomerization quantum yields. The values obtained in hexane for the 11-*cis*- to *all-trans*-retinal process ($\phi_{isom} = 0.25 \pm 0.03$) and *all-trans*- to 13-*cis*-retinal process ($\phi_{isom} = 0.07 \pm 0.03$) are in gratifying agreement with the most recent reported values.^{13,14} These results indicate that the transient changes in optical density at 365 nm accurately reflect the production of isomers. The energy extrapolation procedure (Figure 6) also furnished values of ϕ_{isc} (*all-trans*, 0.62 ± 0.05 in hexane, 0.11 ± 0.03 in methanol; 11-*cis*, 0.50 ± 0.03 in hexane) which we believe to be the most reliable ones to date.

Before describing our evaluation of the triplet extinction coefficients, we need to consider the most recent study of the retinal photoisomerization problem by Menger and Kliger.¹² These authors have found that, for 11-*cis*-retinal in nonpolar solution, the rate of growing in of absorption due to the product isomer (predominantly *all-trans*) matches the decay rate of the triplet absorption. We were able to confirm this result. However, the conclusion of Menger and Kliger that the equality of the isomer growth and triplet decay rates implicates the thermalized triplet state in the isomerization process is untenable. Thus, it is easily shown that these rates will be identical for *any* mechanism, whether or not the thermalized triplet state is involved.³⁴ Since the appearance of absorption due to the isomeric product will always follow exactly the decay of the triplet state, the shape of the oscilloscope traces is determined by the values of the ground-state and triplet-state extinction coefficients at the measurement wavelength. With overlapping absorptions, any trace shape can be produced, as is demonstrated by the step-function trace obtained at 397 nm for 11-*cis*-retinal in hexane (Figure 5). Consequently, the observation of a

step-type trace in methanol does not necessarily indicate a different isomerization mechanism in this solvent.¹² We believe, with Rosenfeld et al.,¹¹ that the insensitivity of ϕ_{isom} to oxygen constitutes compelling evidence against a relaxed triplet state mechanism for the photoisomerization of 11-*cis*-retinal in hexane. The development which follows incorporates this conviction.

The construction of the triplet state absorption spectra from the transient absorption curves of Figure 4 will now be considered. For this and the subsequent discussion, it will be useful to define the following symbols in which time is understood to be variable unless labeled otherwise.

$$\begin{aligned} \Delta D_{\lambda}^0, \Delta D_{\lambda}^{\infty} &= \text{optical density change at wavelength } \lambda \text{ immediately after laser pulse (0) and after complete transient decay } (\infty) \\ \epsilon_{\text{AT-T}}^{\lambda}, \epsilon_{11\text{-T}}^{\lambda} &= \text{molar extinction coefficients at } \lambda \text{ of the triplet states of } \textit{all-trans}\text{- (AT-T) and 11-} \textit{cis}\text{-retinal (11-T)} \\ \epsilon_{\text{AT}}^{\lambda}, \epsilon_{11}^{\lambda} &= \text{molar extinction coefficients at } \lambda \text{ of the corresponding ground states} \\ C_{\text{AT-T}}, C_{11\text{-T}} &= \text{concentrations of the retinal triplet (AT-T, 11-T) and ground (AT,11) states.} \\ C_{\text{AT}}, C_{11} &= \text{concentrations of the retinal ground (AT,11) states.} \\ \text{Superscripts designate } t &= 0, \infty \\ d &= \text{path length, cm} \end{aligned}$$

The sum of the concentrations of the various ground-state and triplet species is taken to be equal to the initial retinal concentration (C_{AT}^0 or C_{11}^0) at all times.³⁵ Since the conditions under which they were measured (low concentration, high pulse energy) assured the complete depletion of the ground states (cf. Figures 2 and 3), the absorption shown in Figure 4 is due only to the triplet states. For *all-trans*-retinal, which has a small ϕ_{isom} value in hexane (~ 0.07), the assumption is made that the transient absorption represents only the triplet state with trans configuration.³⁶ The extinction coefficients $\epsilon_{\text{AT-T}}^{\lambda}$, computed in a straightforward manner from eq 2, are displayed in Figure 7.

$$\Delta D_{\lambda}^0 = C_{\text{AT}}^0 (\epsilon_{\text{AT-T}}^{\lambda} - \epsilon_{\text{AT}}^{\lambda}) d \quad (2)$$

The error in these values, which arises from the neglect of small absorption contributions by triplet states of other configurations, measurement noise, and uncertainties in the initial retinal concentration and in d , and the bandwidth of the monochromator, is estimated as $\pm 10\%$.⁴⁴

In the case of 11-*cis*-retinal in hexane the analysis is more complicated. First of all, we applied the analogue of eq 2 for the 11-*cis* isomer to compute values of an "effective" extinction coefficient $\epsilon_{11\text{-T}}^{\lambda}(\text{eff})$. The results are shown as the dashed curve in Figure 7. We note at once that this spectrum differs in both shape and absolute values from the triplet spectrum of *all-trans*-retinal. Consequently, the proposal that 11-*cis*-retinal, *all-trans*-retinal, and 7-*cis*-retinals all produce the same equilibrated mixture of isomeric triplet states²⁰ is not valid, at least for the 11-*cis* and *all-trans* isomers in hexane. We now consider the question whether or not the "effective" triplet spectrum is due only to the 11-*cis* triplet state. The following observation is pertinent. With total depletion of the 11-*cis*-retinal ground state (Figure 5), the complete decay of the triplet absorption leaves a solution containing a 1.0:1.1 mixture of 11-*cis* and *all-trans* isomers. This ratio was obtained from the measured optical density at 365 nm. Since we have already excluded the relaxed triplet state isomerization mechanism (vide supra), there is no decay of 11-*cis* triplets to *all-trans* triplets. Consequently, the ground-state *all-trans*-retinal molecules must come from the decay of the *all-trans* triplet molecules produced during the laser pulse, and $C_{\text{AT-T}}^0 = C_{\text{AT}}^0$. The "effective" triplet spectrum of 11-*cis*-retinal therefore represents the triplet states of both of these isomers. The ex-

tinction coefficients of the 11-*cis* triplet state, $\epsilon_{11\text{-T}}^{\lambda}$, were extracted from the curve in Figure 4 with aid of eq 3 and 4, in which all other quantities are measured or known.

$$\Delta D_{365}^{\infty} = C_{\text{AT}}^{\infty} (\epsilon_{\text{AT}}^{365} - \epsilon_{11}^{365}) d \quad (3)$$

$$\Delta D_{\lambda}^0 = [C_{11}^0 (\epsilon_{11\text{-T}}^{\lambda} - \epsilon_{11}^{\lambda}) + C_{\text{AT}}^{\infty} (\epsilon_{\text{AT-T}}^{\lambda} - \epsilon_{11\text{-T}}^{\lambda})] d \quad (4)$$

The resulting 11-*cis* triplet spectrum in hexane is shown in Figure 7. The triplet spectra in this figure enable us to glean some information from the step-type oscilloscope trace, observed at 397 nm for 11-*cis*-retinal (Figure 5). At this wavelength, ΔD_{λ}^0 is constant between $t = 0$ and ∞ .

$$\begin{aligned} \Delta D_{\lambda}^0 &= [C_{\text{AT}} (\epsilon_{\text{AT}}^{\lambda} - \epsilon_{11}^{\lambda}) + C_{\text{AT-T}} (\epsilon_{\text{AT-T}}^{\lambda} - \epsilon_{11}^{\lambda}) \\ &\quad + C_{11\text{-T}} (\epsilon_{11\text{-T}}^{\lambda} - \epsilon_{11}^{\lambda})] d \quad (5) \end{aligned}$$

The triplet spectra of Figure 7 indicate that, within experimental error, the isosbestic points for both *all-trans*- and 11-*cis*-retinal and their respective triplet states appear near 397 nm. Then $\Delta D_{\lambda}^0 = (C_{\text{AT}} + C_{\text{AT-T}}) (\epsilon_{\text{AT}}^{\lambda} - \epsilon_{11}^{\lambda}) d$, and eq 5 shows that the sum $C_{\text{AT}} + C_{\text{AT-T}}$ is constant. Thus, the invariance with time of ΔD_{397} signifies the match between the decrease of the *all-trans* triplet state concentration and the increase of the ground-state concentration. For the points $t = 0$ and $t = \infty$, eq 5 gives $C_{\text{AT}}^{\infty} - C_{\text{AT}}^0 = C_{\text{AT-T}}^0$, where C_{AT}^0 is the concentration of the *all-trans* ground state immediately after the laser pulse. Since triplet state is present at that time ($C_{\text{AT-T}}^0 \neq 0$), some but not all ground state *all-trans*-retinal molecules can be produced during the laser pulse.

The evidence presented to this point, and that reported by others,^{11,12} is compatible with the following photoisomerization pathways.

(A) Singlet mechanism 1: The first excited singlet (S_1) state of 11-*cis*-retinal is converted to an S_1 state with a trans configuration. These two S_1 states, which are separated by a low rotation barrier, decay to their respective ground states.³⁷

(B) Singlet mechanism 2: The S_1 state of 11-*cis*-retinal internally converts to a hot ground state which partitions between relaxed 11-*cis* and *all-trans* configurations.

(C) Triplet mechanism:¹¹ Intersystem crossing from S_1 ultimately yields an internally excited first triplet (T_1^*) state which relaxes into T_1 states with 11-*cis* and *all-trans* configurations.³⁸

A key difference between the singlet (A and B) and triplet pathways is the presence or absence of ground-state *all-trans*-retinal molecules immediately after the pulse. Thus, mechanisms A and B predict that $C_{\text{AT}}^0 \neq 0$, and mechanism C that $C_{\text{AT}}^0 = 0$. A nonzero C_{AT}^0 value may, of course, mean that both paths are followed. These predictions are amenable to direct experimental testing by means of transient absorption measurements at 445 nm (triplet production at $t = 0$) and 365 nm (*all-trans*-retinal production at $t = 0$ and ∞). The pertinent equations are

$$\Delta D_{445}^0 = (\epsilon_{\text{AT-T}}^{445} C_{\text{AT-T}}^0 + \epsilon_{11\text{-T}}^{445} C_{11\text{-T}}^0) d$$

$$\Delta D_{365}^0 = [\Delta \epsilon C_{\text{AT}}^0 + \Delta \epsilon_{\text{AT-T}} C_{\text{AT-T}}^0 + \Delta \epsilon_{11\text{-T}} C_{11\text{-T}}^0] d \quad (6)$$

$$\Delta D_{365}^{\infty} = \Delta \epsilon (C_{\text{AT}}^0 + C_{\text{AT-T}}^0) d$$

where, for convenience, $\Delta \epsilon = \epsilon_{\text{AT}}^{365} - \epsilon_{11}^{365}$, $\Delta \epsilon_{\text{AT-T}} = \epsilon_{\text{AT-T}}^{365} - \epsilon_{11}^{365}$, and $\Delta \epsilon_{11\text{-T}} = \epsilon_{11\text{-T}}^{365} - \epsilon_{11}^{365}$. Measurements of ΔD_{λ} were made for a 1.0×10^{-5} M solution of 11-*cis*-retinal at various energies (Figure 8) and, using the known values of the extinction coefficients, eq 6 were solved for C_{AT}^0 , $C_{\text{AT-T}}^0$, and $C_{11\text{-T}}^0$, the concentrations of ground-state *all-trans*-retinal, the *all-trans* triplet, and the 11-*cis* triplet which are present immediately after cessation of the excitation. The results of these computations are displayed in Figure 9. With an uncertainty of ca. $\pm 1 \times 10^{-6}$ M³⁹ we find that, at all energies, essentially equal

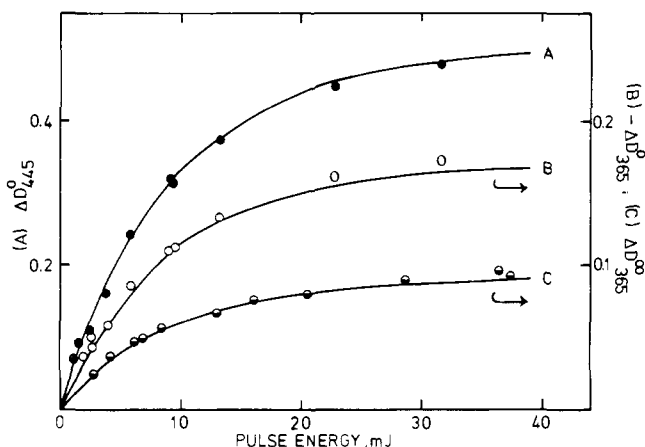


Figure 8. Changes in optical density for 1.0×10^{-5} M 11-*cis*-retinal in degassed *n*-hexane. (A) At 445 nm, $t = 0$; (B) at 365 nm, $t = 0$; (C) at 365 nm, $t = \infty$. The solid curves were computed for the scheme of Figure 10; see text.

amounts of 11-*cis* and all-*trans* triplets are produced and C_{AT}^0 is zero.

To interpret these results, we must consider how the concentrations C_{AT}^0 , C_{AT-T}^0 , and C_{11-T}^0 would vary for the singlet mechanisms. Qualitatively, one can see that C_{AT}^0 will pass through a maximum since the all-*trans* ground state will be converted to its triplet state in proportion to the intensity of the excitation pulse. For a quantitative comparison of the mechanisms, we have used a previously described method^{22,29} to numerically integrate the differential equations describing the various photophysical and photochemical processes involved in them over a time interval which encompasses the duration of the laser pulse. The input parameters for these calculations are the excited singlet and triplet state lifetimes, ϕ_{isc} , ϕ_{isom} , and the extinction coefficients of the 11-*cis*- and all-*trans*-retinal ground and triplet states. The ϕ_{isc} value for 11-*cis*-retinal refers to the total (11-*cis* and all-*trans*) triplet yield. Inclusion of a picosecond $S_1 \rightarrow S_n$ absorption process⁴⁰ was found not to affect these simulations. The dashed curve in Figure 9 represents the computed variation of the postpulse all-*trans*-retinal concentration C_{AT}^0 with energy for singlet pathway B, which falls barely within the uncertainty range of these values. Moreover, the ratio $\Delta D_{365}^0 / \Delta D_{445}^0$, which is measured to be constant with energy ($\pm 10\%$ at 5 mJ/pulse, $\pm 5\%$ at 30 mJ/pulse), is predicted to decrease by 18% between 5 and 30 mJ/pulse for singlet mechanism B and by 16% for mechanism A. The ratio $\Delta D_{365}^0 / \Delta D_{445}^0$ shows a similar discrepancy between observed and computed values. Mechanism C predicts these ratios to vary by no more than 4% in this energy range.

These findings permit us to exclude singlet mechanisms A and B as major pathways, and to conclude that the direct photoisomerization of 11-*cis*-retinal in hydrocarbon solvents occurs predominantly by the nonrelaxed triplet state mechanism C which was originally proposed by Rosenfeld et al.¹¹ for the triplet-sensitized isomerization.

According to this mechanism, 11-*cis*-retinal forms both the 11-*cis* and all-*trans* relaxed triplet states during the laser pulse, and the ground-state all-*trans*-retinal molecules come from the decay of the latter, i.e., $C_{AT}^0 = C_{AT-T}^0$. Moreover, mechanism C predicts that the ratio of triplet concentrations, C_{AT-T}^0 / C_{11-T}^0 , remains constant with increasing excitation intensity. Measurements of ΔD_{365}^0 at low 11-*cis*-retinal concentration and high pulse energies show that this is not exactly the case, and that this ratio increases slightly with energy. We ascribe this behavior to a small, energy-dependent biphotonic contribution to the isomerization which is considered to operate as follows. Since the excited singlet state lifetimes are short (~ 20 ps⁴⁰),

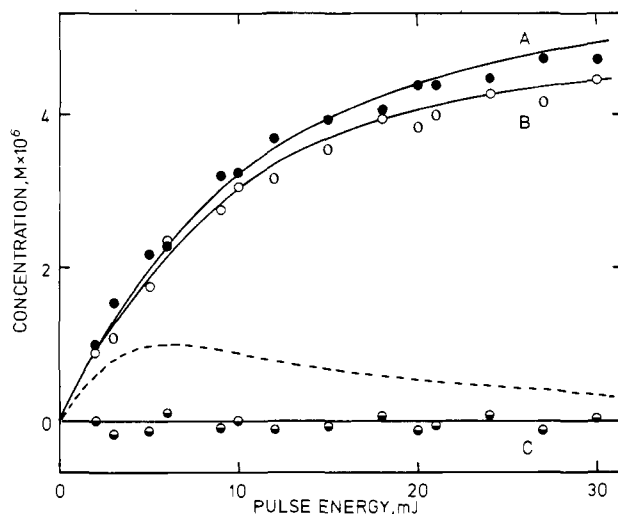


Figure 9. Variation with energy of the concentrations at $t = 0$ of all-*trans* triplet state (C_{AT-T}^0) (A), 11-*cis* triplet state (C_{11-T}^0) (B), and all-*trans*-retinal ground state (C_{AT}^0) (C), in the 11-*cis*-retinal solution of Figure 8. The solid curves were computed with the model of Figure 10, for which $C_{AT}^0 = 0$ at all energies. The broken curve represents the variation of C_{AT}^0 for singlet pathway B; see text.

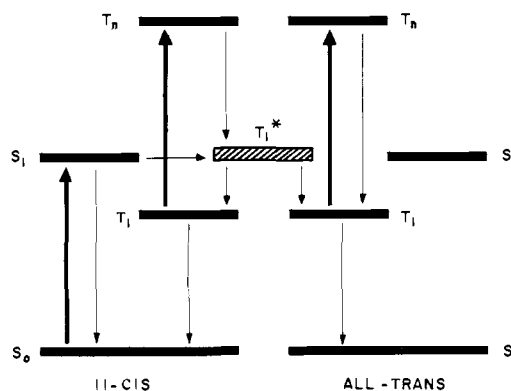


Figure 10. Photoisomerization scheme for 11-*cis*-retinal. The heavy arrows represent the excitations, and T_1^* the internally excited triplet state.

the thermalizing relaxations very rapid, and triplet lifetimes relatively long (~ 10 μ s^{11,16,20}), the triplet concentrations during the ~ 25 -ns laser pulse will be substantial. Figure 7 shows that both the 11-*cis*- and all-*trans*-retinal triplet states absorb 347-nm radiation. This absorption will populate the upper triplet levels (T_n) of the two isomers. For the 11-*cis* isomer, internal conversion will lead to the nonrelaxed T_1 level from which partitioning into 11-*cis* and all-*trans* T_1 configurations occurs. Since the photoisomerization of all-*trans*-retinal does not produce the 11-*cis* isomer,¹⁴ the all-*trans* T_n state is presumed to revert predominantly to the relaxed all-*trans* T_1 state; some possible diversion to the 13-*cis* T_1 state is neglected.

The proposed photoisomerization scheme for 11-*cis*-retinal in hydrocarbon solvents, including this biphotonic process, is summarized in Figure 10. The solid curves in Figures 8 and 9 were computed for this model. In both cases the agreement between the calculated and observed values is seen to be good.

Finally, we consider the relation of these results for 11-*cis*-retinal to the triplet-sensitized isomerization and the direct photoisomerization of other isomers. While the same basic mechanism is considered to be operative in the sensitized and direct isomerizations of 11-*cis*-retinal, the partitioning of the nonrelaxed triplet intermediate into *cis* and *trans* configura-

tions is distinctly different in the two cases. With $\phi_{isc} = 0.5$ and $\phi_{isom} = 0.25$ for direct excitation, 50% of the intermediate triplet state is converted to the trans form, whereas for the sensitized reaction (${}^3\phi_{isom} = 0.15-0.17^{11,13}$) only ca. 15% follows this channel. A reasonable interpretation of this finding is that, as anticipated by Rosenfeld et al.,¹¹ the two excitation modes populate different triplet vibronic levels, and that the relaxation of these states to cis and trans configurations is governed by their energy content. The excitation wavelength dependence reported for the ϕ_{isom} of 11-*cis*-retinal⁹ is consistent with an energy-dependent partitioning mode.

Evidently, the photoisomerization pathway followed by a particular retinal isomer is decisively influenced by the detailed shapes of the excited state potential energy surfaces for that configuration. Consequently, no meaningful mechanistic conclusions about the other isomers can be drawn from the results for 11-*cis*-retinal. A case in point is *all-trans*-retinal, the behavior of which is quite different from that of the 11-*cis* isomer. Not only is ϕ_{isom} much smaller for the direct isomerization of the trans compound which produces no 11-*cis* isomer but also, its isomerization cannot be sensitized by triplet energy transfer.^{11,13} If the same isomerization mechanism is followed as for 11-*cis*-retinal, the *all-trans* and 11-*cis* triplet state manifolds are not coupled and, as suggested by Menger and Kliger,¹² the reactive triplet level is not populated by the sensitizer. The quantum yields and product distributions are significantly modified by the nature of the solvent.^{14,41} Thus, for all the retinal isomers, the isomerization mechanism may change with the environment, which can affect ground-state conformations and the ordering of the excited states.^{30,42,43} Since they have ϕ_{isom} values of reasonable magnitude in hydrocarbon solution,¹³ 13-*cis*- and 9-*cis*-retinal may be amenable to study by the same method we have used for 11-*cis*-retinal.

Summary

In this study we have shown that the transient absorption of 11-*cis*-retinal is due to both the 11-*cis* and *all-trans* triplet states. Working at laser excitation energies which produce complete ground-state depletion, we were able to construct the complete triplet spectra of these isomers in the 300–500-nm region. With this information and the results of measurements in the ground-state and triplet-state absorption regions at various energies and times after excitation, it could be shown that, within experimental error, little or no *all-trans*-retinal appears to be produced during the laser pulse. This result, and quantitative absorption and concentration calculations based on kinetic models, indicate the applicability of the nonrelaxed triplet state pathway proposed by Rosenfeld et al.¹¹ to the direct photoisomerization of 11-*cis*-retinal in hydrocarbon solvents.

Acknowledgments. The research was supported by NIH Research Grant R01 ES00376 awarded by the National Institute of Environmental Health Sciences and, in part, by Grant RR07143, PHS/DHW. We are grateful to Mr. D. Rust III for his assistance with the instrumental aspects of this work, and to Professor Ralph Becker for valuable comments.

References and Notes

- (1) To whom correspondence should be addressed.
- (2) A. Lewis R. Fager, and E. W. Abrahamson, *J. Raman Spectrosc.*, **1**, 465 (1973).
- (3) A. R. Oseroff and R. H. Callender, *Biochemistry*, **13**, 4243 (1974).
- (4) R. Mathies, A. R. Oseroff, and L. Stryer, *Proc. Natl. Acad. Sci. U.S.A.*, **73**, 1 (1976).
- (5) R. H. Callender, A. Doukas, R. Crouch, and K. Nakanishi, *Biochemistry*, **15**, 1621 (1976).
- (6) R. Hubbard and G. Wald, *J. Gen. Physiol.*, **36**, 269 (1952).
- (7) For a recent review, see B. Honig and T. G. Ebrey, *Annu. Rev. Biophys. Bioeng.*, **3**, 151 (1974); and *Acc. Chem. Res.*, **3**, 81–112 (1975), which is devoted to the chemistry of vision.

- (8) R. S. Becker, G. Hug, P. K. Das, A. M. Schaffer, T. Takemura, N. Yamamoto, and W. Waddell, *J. Phys. Chem.*, **80**, 2265 (1976).
- (9) A. Kropf and R. Hubbard, *Photochem. Photobiol.*, **12**, 249 (1970).
- (10) R. A. Raubach and A. V. Guzzo, *J. Phys. Chem.*, **77**, 889 (1973).
- (11) T. Rosenfeld, A. Alchalel, and M. Ottolenghi, *J. Phys. Chem.*, **78**, 336 (1974).
- (12) E. L. Menger and D. S. Kliger, *J. Am. Chem. Soc.*, **98**, 3975 (1976).
- (13) W. H. Waddell, R. Crouch, K. Nakanishi, and N. J. Turro, *J. Am. Chem. Soc.*, **98**, 4189 (1976).
- (14) W. H. Waddell and D. L. Hopkins, *J. Am. Chem. Soc.*, in press.
- (15) R. Bensasson, E. J. Land, and T. G. Truscott, *Photochem. Photobiol.*, **17**, 53 (1973).
- (16) M. M. Fisher and K. Weiss, *Photochem. Photobiol.*, **20**, 423 (1974).
- (17) R. Bensasson, E. J. Land, and T. G. Truscott, *Photochem. Photobiol.*, **21**, 419 (1975).
- (18) In polar solution (e.g., methanol), the intersystem crossing quantum efficiency is significantly lower (~ 0.1); cf. ref 16.
- (19) The value of $\phi_{isom} = 0.75$ for the biacetyl-sensitized isomerization of 11-*cis*-retinol reported in ref 10 is evidently too high.
- (20) A. Harriman and R. S. H. Liu, *Photochem. Photobiol.*, **26**, 29 (1977).
- (21) R. H. Dekker, B. N. Srinivasan, J. R. Huber, and K. Weiss, *Photochem. Photobiol.*, **18**, 457 (1973).
- (22) M. S. Grodowski, B. Veyret, and K. Weiss, *Photochem. Photobiol.*, **26**, 341 (1977).
- (23) C. A. Parker and W. T. Rees, *Analyst*, **85**, 587 (1960).
- (24) (a) G. Weber and F. W. J. Teale, *Trans. Faraday Soc.*, **53**, 646 (1957); (b) I. B. Berlman, "Handbook of Fluorescence Spectra of Aromatic Molecules", 2nd ed, Academic Press, New York, N.Y., 1971, pp 364, 412.
- (25) A. V. Buettner, B. B. Snavely, and O. G. Peterson, "Molecular Luminescence", E. Lim, Ed., W. A. Benjamin, New York, N.Y., 1969, pp 403–422.
- (26) B. Amand and R. Bensasson, *Chem. Phys. Lett.*, **34**, 44 (1975).
- (27) R. Bensasson and E. J. Land, *Trans. Faraday Soc.*, **67**, 1904 (1971).
- (28) W. M. Moreau, T. A. Tyler, and K. Weiss, *J. Chem. Educ.*, **43**, 435 (1966).
- (29) M. M. Fisher, B. Veyret, and K. Weiss, *Chem. Phys. Lett.*, **28**, 60 (1974).
- (30) T. Takemura, P. K. Das, G. Hug, and R. S. Becker, *J. Am. Chem. Soc.*, **98**, 7099 (1976).
- (31) W. H. Waddell, A. M. Schaffer, and R. S. Becker, *J. Am. Chem. Soc.*, **95**, 8223 (1973).
- (32) R. Azerad, R. Bensasson, M. B. Cooper, E. A. Dawe, and E. J. Land, "Excited States of Biological Molecules", J. B. Birks, Ed., Wiley, New York, N.Y., 1976, pp 531–539.
- (33) These results were obtained with a conventional dc fluorimeter; cf. A. M. Halpern and R. M. Danziger, *Chem. Phys. Lett.*, **16**, 72 (1972).
- (34) In the general case, the change in optical density (ΔD) in the ground state absorption region is, with unit path length, given by

$$\Delta D = \epsilon_{11}C_{11} + \epsilon_{AT}C_{AT} + \epsilon_T C_T - \epsilon_{11}C_0 \quad (i)$$

where ϵ and C represent the extinction coefficients and concentrations, respectively, the subscripts 11, AT, and T designate the 11-*cis* isomer, *all-trans* isomer, and triplet state, respectively. With the sum of concentrations equal to the initial concentration (C_0) of 11-*cis*-retinal at all times ($C_0 = C_{11} + C_{AT} + C_T$), and an exponential decay of the triplet state with rate constant k , eq i yields

$$\Delta D = (C_{AT}^0 + C_{AT}^T)\Delta\epsilon + (\Delta\epsilon_T C_T^0 - \Delta\epsilon C_{AT}^T)e^{-kt} \quad (ii)$$

and the rate law

$$-d\Delta D/dt = (\Delta\epsilon_T C_T^0 - \Delta\epsilon C_{AT}^T)ke^{-kt} \quad (iii)$$

In these equations, $\Delta\epsilon = \epsilon_{AT} - \epsilon_{11}$ and $\Delta\epsilon_T = \epsilon_T - \epsilon_{11}$, C_{AT}^0 and C_{AT}^T are the concentrations of the *all-trans* isomer present immediately after the pulse (i.e., produced during the pulse) and formed at $t = \infty$ by triplet decay, respectively, and C_T^0 is the initial triplet concentration. Equations ii and iii clearly accommodate mechanisms in which C_{AT}^T is nonzero and zero; the same exponential rate law, $\ln \{(\Delta D_0 - \Delta D_\infty)/(\Delta D - \Delta D_\infty)\} = kt$, where $\Delta D_0 = \Delta\epsilon C_{AT}^0 + \Delta\epsilon_T C_T^0$ and $\Delta D_\infty = \Delta\epsilon(C_{AT}^0 + C_{AT}^T)$, is obeyed in both cases. The assumption made by Menger and Kliger¹² in the analysis of their data, that the transients generated from 11-*cis*-retinal have negligible absorption in the region (370–380 nm) where the ground state absorbs strongly, though shown to be erroneous in our experiments (cf. Figure 7), does not affect the above conclusion.

- (35) High-energy laser excitation with transient measurements near 300 nm, where the pertinent retinal isomers show an isosbestic point,⁹ bear out the validity of this assumption. On the other hand, prolonged irradiation with a xenon arc lamp causes the irreversible formation of products which absorb below 300 nm.
- (36) Consistent with this ϕ_{isom} value, measurements at 365 nm after complete transient decay indicate $<10\%$ conversion to the 13-*cis* isomer. This assumption is necessary since no meaningful correction can be made for an absorption due to the 13-*cis* triplet state.
- (37) R. S. Becker, K. Inuzuka, J. King, and D. E. Balke, *J. Am. Chem. Soc.*, **93**, 43 (1971). Since no 11-*cis* isomer but a small yield of 13-*cis* isomer is formed from *all-trans*-retinal, the barrier separating the trans configuration S_1 state from a 13-*cis* configuration is presumably lower than the one between the trans and 11-*cis* configurations.
- (38) A referee has suggested that the isomerization may occur in a higher electronic triplet level. The T_2 (π, π^*) state, for which substantial cis \rightleftharpoons trans rotation barriers have been calculated,³⁷ is unlikely to be directly involved in the isomerization,¹¹ but participation of the lowest n, π^* triplet state, about which little is known, cannot be ruled out.
- (39) The uncertainty in the concentrations was estimated by first determining the mean error in ΔD from the best smooth curves drawn to fit the exper-

imental points of Figure 8, and then applying a propagation of errors treatment. In this analysis, the extinction coefficients were considered to be constant since arbitrary variations of a few percent result in physically unrealistic concentrations (large negative values and/or sums which substantially exceed the initial ground-state concentration).

- (40) R. M. Hochstrasser, D. L. Narva, and A. C. Nelson, *Chem. Phys. Lett.*, **43**, 15 (1976).
 (41) M. Denny and R. S. H. Liu, *J. Am. Chem. Soc.*, **99**, 4865 (1977).
 (42) R. R. Birge, K. Schulten, and M. Karplus, *Chem. Phys. Lett.*, **31**, 451 (1975).

(43) R. R. Birge, M. J. Sullivan, and B. E. Kohler, *J. Am. Chem. Soc.*, **98**, 358 (1976).

(44) After this manuscript was completed, a paper appeared (R. Bensasson, E. A. Dawe, D. A. Long, and E. J. Land, *J. Chem. Soc., Faraday Trans. 1*, **73**, 1319 (1977)) which reports $\epsilon_{AT-T}^{445} = 1.14 \times 10^5 \text{ M}^{-1} \text{ cm}^{-1} (\pm 15\%)$ in *n*-hexane. While we are unable to account for the large discrepancy between this value, which was determined by a pulse radiolysis-energy transfer technique, and ours of $7.0 \times 10^4 \text{ M}^{-1} \text{ cm}^{-1} (\pm 10\%)$, we may note that the higher value is inconsistent with the saturation of triplet state absorption at relatively low laser pulse energies (Figure 2).

Detection and Investigation of Allyl and Benzyl Radicals by Photoelectron Spectroscopy

F. A. Houle and J. L. Beauchamp*

Contribution No. 5686 from the Arthur Amos Noyes Laboratory of Chemical Physics, California Institute of Technology, Pasadena, California 91125. Received October 17, 1977

Abstract: Allyl and benzyl radicals have been produced by pyrolysis in a photoelectron spectrometer. Adiabatic and vertical IPs coincide for both species and are determined to be $8.13 \pm 0.02 \text{ eV}$ for allyl, $7.20 \pm 0.02 \text{ eV}$ for benzyl, and $7.22 \pm 0.02 \text{ eV}$ for benzyl- α - d_2 . Heats of formation derived from these results are $225.5 \pm 1.1 \text{ kcal/mol}$ for allyl cation and $211 \pm 1.1 \text{ kcal/mol}$ for benzyl cation. Vibrational structure has been resolved. The results are discussed in terms of the role of the unpaired electron in the conjugated π systems of these radicals.

Application of various spectroscopic techniques to free radicals has provided a great deal of information on their electronic structure, geometries, spin densities, and normal modes. Recently, photoelectron spectroscopy (PES) has been added to the list of techniques available, allowing characterization of the relationship between the radical and its ion. In particular, the first photoelectron band yields information on the unpaired electron in the radical. Much can be learned about the localization and bonding character of this electron by consideration of the shape of the band itself, especially when vibrational structure is present. The information obtained can be combined with that from other sources such as electron spin resonance spectroscopy (ESR) and theoretical calculations to characterize stabilities and reactivities of these transient species. Radicals having conjugated π systems are particularly well studied. Allyl and benzyl radicals are among the simplest and best understood of these, and are the subject of the present work.

Both of these species have been treated in numerous theoretical calculations.¹ Many of these involve interpretation of ESR hyperfine splittings²⁻⁵ in terms of spin densities, which give information on the delocalization of the unpaired electron. In allyl radical,^{2,3} the positive density is found entirely on the equivalent terminal carbon atoms, with a small negative component on the central carbon. In benzyl radical,^{4,5} on the other hand, the spin density on the exo methylene is $\sim 0.7-0.8$, the remainder being shared between the ortho and para positions on the phenyl ring. The distribution of unpaired spin in these two radicals can be understood qualitatively in terms of valence bond resonance structures.

Theoretical effort has also been directed toward an understanding of the electronic structure of allyl⁶⁻⁹ and benzyl¹⁰⁻¹³ radicals. Analyses of the absorption and emission spectra of benzyl radical have identified the symmetries of the states involved, as well as most of the normal modes in the ground state.¹⁰⁻¹³ However, owing to the large number of electrons in benzyl radical, only allyl radical has been the subject of ab initio calculations involving large basis sets.⁶⁻⁹

Both molecular orbital⁶⁻⁸ and generalized valence bond

(GVB)⁷⁻⁹ calculations indicate that the unpaired electron in allyl radical is mainly nonbonding. Levin and Goddard^{7,8} found that this species is reasonably well described using wave functions of an ethylene molecule fused to methylene. Removal of this electron to form a carbonium ion allows the two remaining π electrons to delocalize over all three centers.¹⁴ This increased delocalization is expected to increase the resonance energy of the ion relative to that of the neutral.¹⁵

The results of the present work are consistent with the spin density distributions derived from ESR studies. They also support the theoretical description of allyl radical discussed above, and indicate that a similar one is appropriate for benzyl radical.

Experimental Section

These experiments are part of a series of studies of free radicals produced by pyrolysis of alkyl nitrites. The instrumentation, which has been briefly described in a previous communication,¹⁶ consists of a photoelectron spectrometer of standard design which has been specifically modified to study the products of gas-phase pyrolyses. A schematic of the spectrometer is shown in Figure 1. The differentially pumped source chamber, 127° electrostatic analyzer, and Channeltron electron multiplier are situated on a stainless steel baseplate in a high-vacuum chamber. The HeI capillary discharge lamp, located directly underneath the source chamber, is separated from the main vacuum chamber by a stage of differential pumping. The analyzer is protected from magnetic fields by a mumetal shield and a set of six Helmholtz coils. Sample gases are introduced into the source chamber through a stainless steel inlet system divided into three sections. Two of these are connected to the bottom of the source chamber and are used for calibrant gases (usually argon) and samples at room temperature. The third enters the vacuum chamber through the side wall. It consists of a 3-mm i.d. quartz tube fitted to a stainless steel flange. This tube is used for pyrolysis. A 2-cm long section at the free end of the tube is wrapped with double-stranded Semflex heater wire insulated with MgO and an Inconel outer sheath. A chromel-constantan thermocouple is wedged between the sheath and the quartz tube to monitor the temperature. Constant temperatures of up to 1000 °C can be maintained for hours. The analyzer is protected from blackbody radiation by a water-cooled copper shield surrounding the hot section. The tip of the quartz tube is inserted through an aperture in the side